Electronic Supplementary Material (ESI) for Inorganic Chemistry Frontiers.

Gelation-induced controlled synthesis of TiO_2 with tunable phase transition for efficient photocatalytic hydrogen evolution

Wenwei Lei, *[a] Ying Wang,[a] Hongji Wang ,[a] Norihiro Suzuki ,[b] Chiaki Terashima *[c] and Akira Fujishima[c]

[a] Hebei Key Laboratory of Nano-biotechnology, School of Environmental and Chemical Engineering, Yanshan University, Qinhuangdao 066004, Hebei, China

[b] Department of Natural Sciences, School of Engineering, Tokyo Denki University, 5 Senjyu Asahi-cho, Adachi-ku, Tokyo 120-8551, Japan

[c] Research Center for Space System Innovation, Tokyo University of Science, 2641 Yamazaki, Noda, Chiba 278-8510, Japan

[d] Institute of Photochemistry and Photomaterials, University of Shanghai for Science and Technology, Shanghai 2000093, P.R. China

Corresponding Authors.

E-mail: leiww@ysu.edu.cn (Wenwei Lei); terashima@rs.tus.ac.jp (Terashima)

Table of Contents

1. Supplemental Methods

Materials: Commercial P25 was obtained from Degussa (Germany). Polyvinyl alcohol (PVA, average Mw 130,000, 99+% hydrolyzed) was obtained from Sigma–Aldrich. N-methyl pyrrolidone (NMP) was obtained from TCI. $TiCl_4$ was obtained from Wako. All the chemicals used without further purification.

Characterization：

The obtained catalysts were characterized morphologically and structurally by field emission scanning electron microscopy (FE-SEM; JSM-7600 F, JEOL, Japan) as well as transmission electron microscopy. The phase structure changes of the catalysts were investigated by X-ray diffractometer (XRD; Ultima IV, Rigaku, Japan) and Raman scattering spectrometer (NRS-5100, Jasco, Japan). Ultraviolet-visible-near-infrared (UV-vis-NIR) spectra were performed with a JASCO V-670 spectrophotometer. The surface elemental composition and changes were analyzed by XPS (ESCA-3400, Shimadzu, Japan). The photocurrent density of the catalyst films was measured with a constant potential meter (Versa STAT 4, METEK, USA) under a three-electrode system at a constant voltage of 0.8 V. The catalyst films were analyzed by XPS (ESCA-3400, Shimadzu, Japan). Silver/silver chloride and platinum wires were used as reference and counter electrodes, respectively. The electrolyte solution was 0.5 M Na_2SO_4. A thin film of catalyst for the working electrode was prepared by sonication by dispersing 20 mg of catalyst into 5 mL of 95 v/v% ethanol. Then 3 mL of the mixture was dropped onto fluorine-doped tin oxide (FTO) glass, and the catalyst was homogeneously dispersed onto the FTO surface by the scraping method. The catalyst-modified FTO glass was then dried at 70 °C for 24 hours.

2. Supplementary Figures

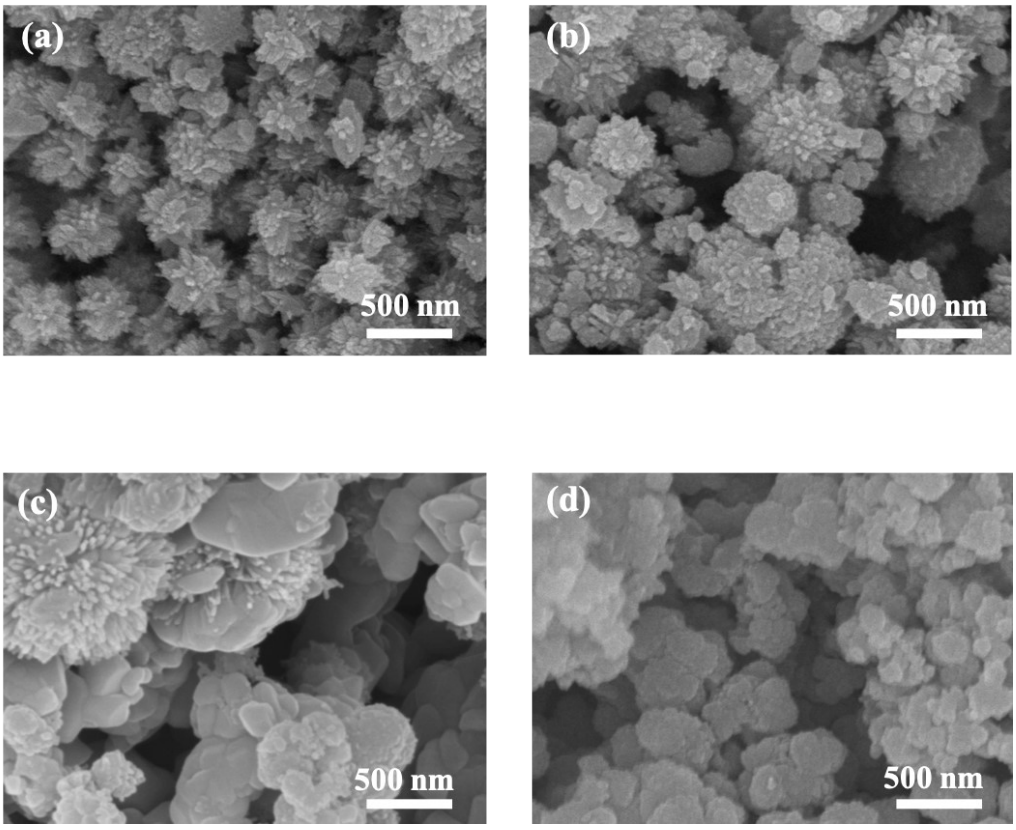

Fig. S1. The SEM images of (a) A_{100}-TiO_2, (b) A_{92}/R_8-TiO_2 (c) A_{44}/R_{56}-TiO_2 and (d) A_7/R_{93}-TiO_2

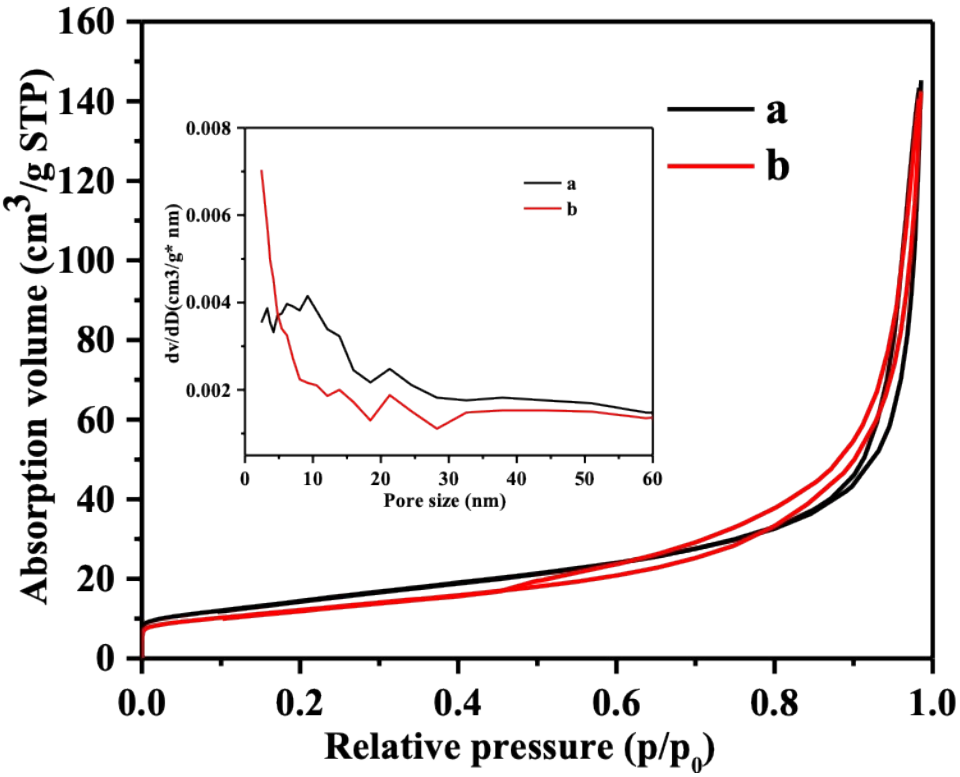

Fig. S2. The nitrogen adsorption–desorption isotherms of (a) the commercial P25 and (b) A_{76}/R_{24}-TiO_2. The insets image is the corresponding pore size distribution curves.

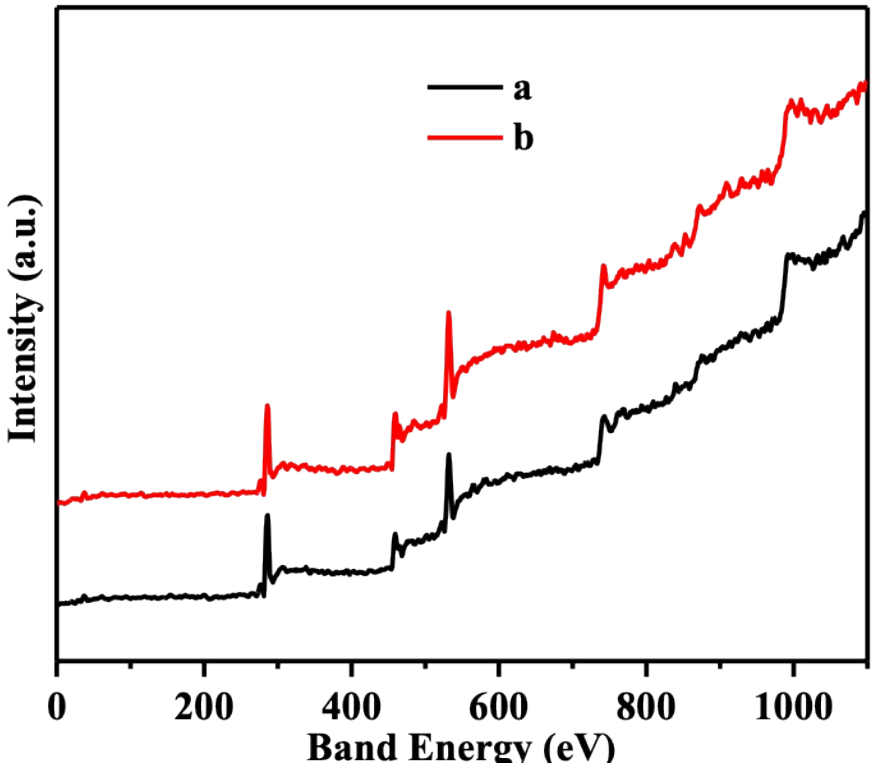

Fig. S3. The full X-ray photoelectron spectra (XPS) spectra of (a) the commercial P25 and (b) A_{76}/R_{24}-TiO_2.

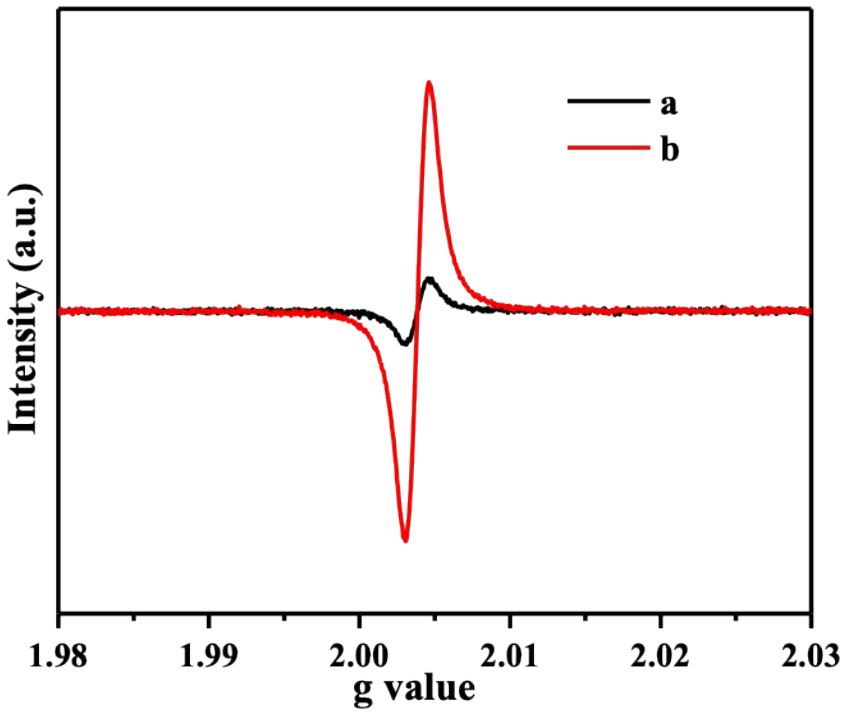

Fig. S4. The EPR spectra measured at room temperature of (a) the commercial P25 and (b) A_{76}/R_{24}-TiO_2.

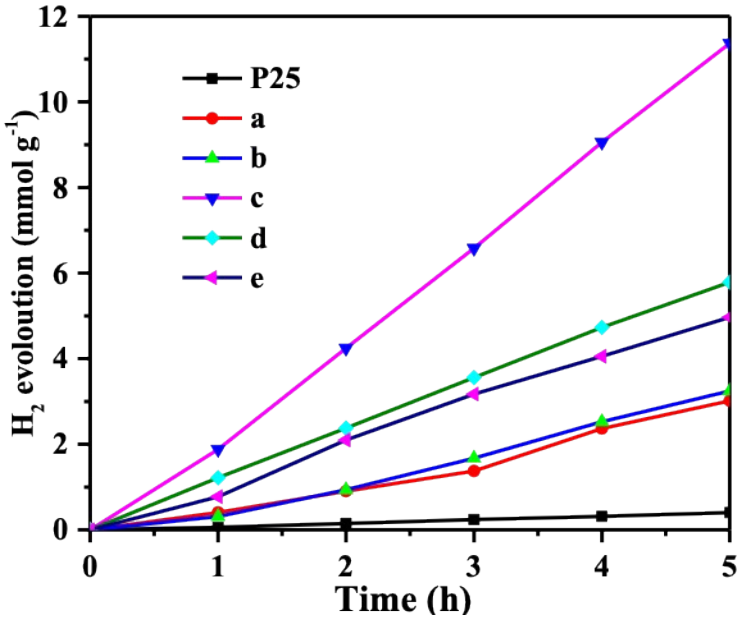

Fig. S5. Hydrogen production from various TiO_2 photocatalysts as a function of time under AM 1.5 light irradiation, (a) A_{100}-TiO_2, (b) A_{92}/R_8- TiO_2, (c) A_{76}/R_{24}- TiO_2, (d) A_{44}/R_{56}- TiO_2, and (e) A_7/R_{93}- TiO_2.

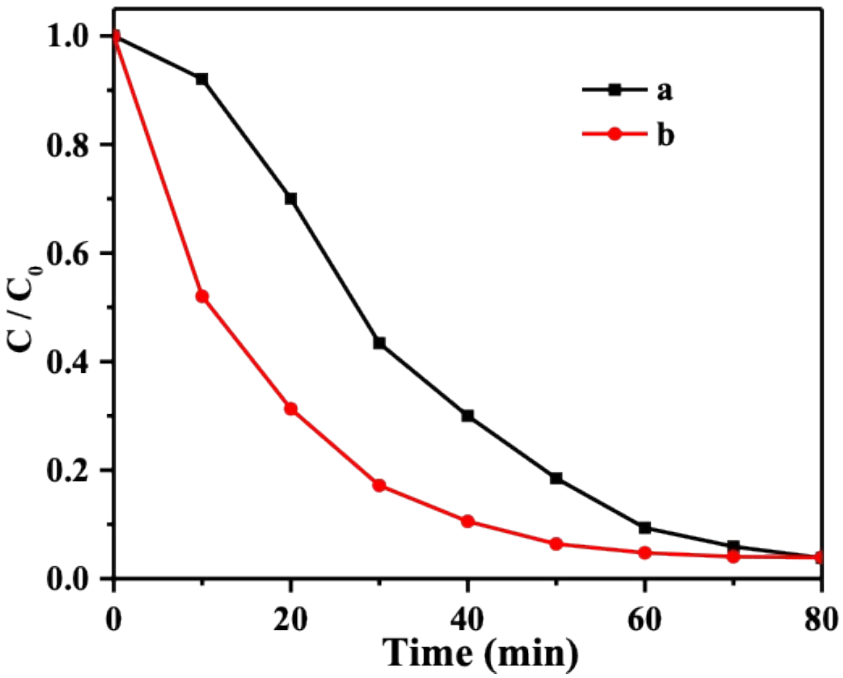

Fig. S6. The photocatalytic decomposition of methylene blue (10 mg L^{-1}) use (a) the commercial P25 and (b) A_{76}/R_{24}-TiO_2.

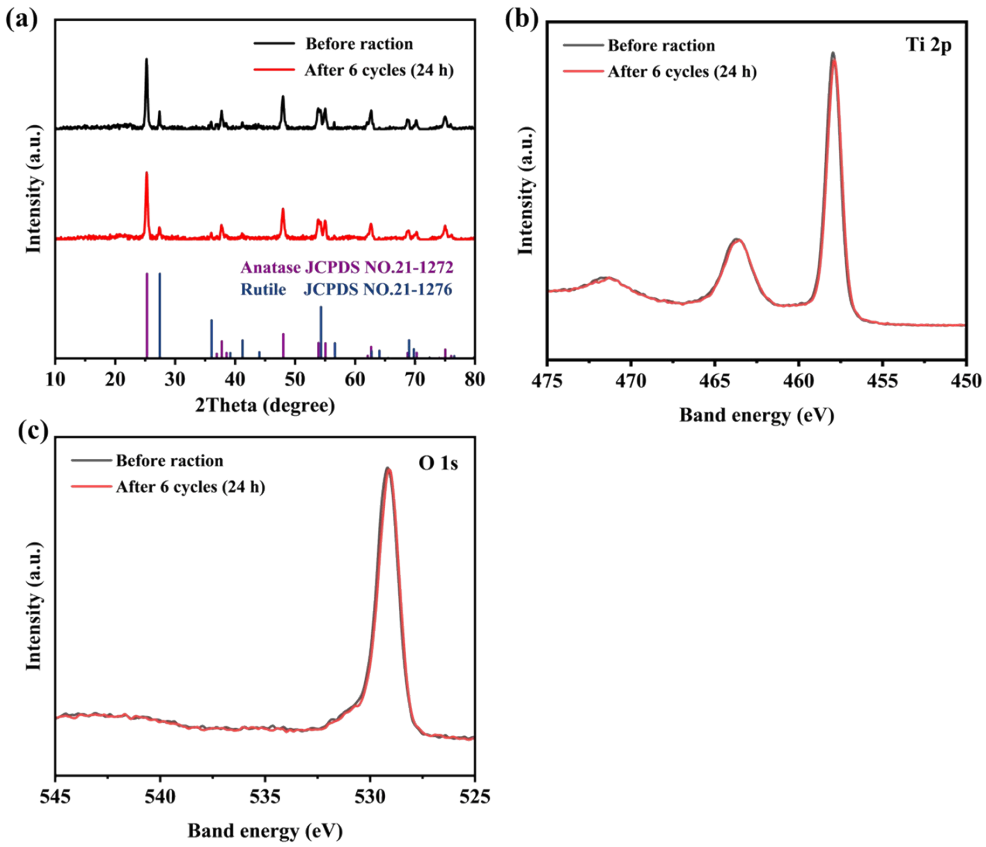

Fig.S7. XRD and XPS tests of A_{76}/R_{24}-TiO_2 before and after 6 cycles (24h) of photocatalytic H_2 production. (a) XRD patterns; High-resolution Ti 2p (b) and O1s (c) XPS spectra.

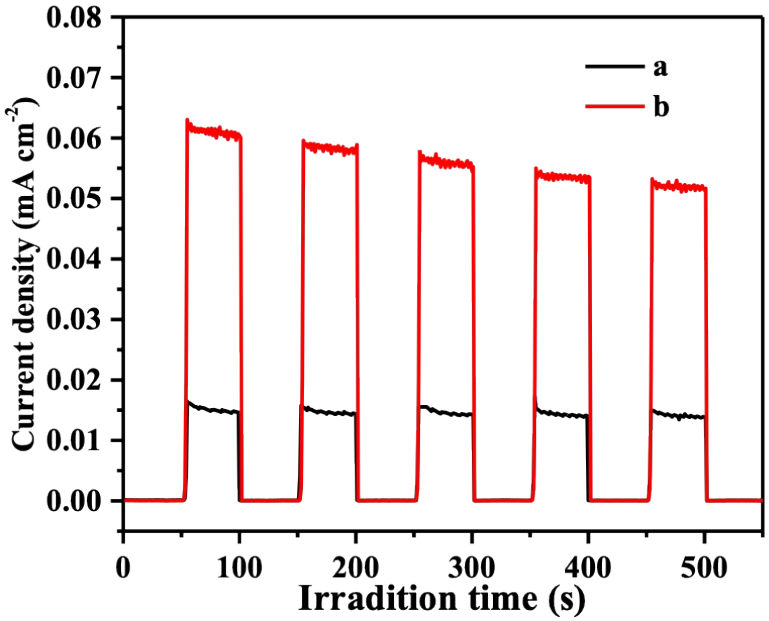

Fig. S8. The photoelectrochemical responses of (a) the commercial P25 and (b) A_{76}/R_{24}-TiO_2 under AM1.5 irradiation.

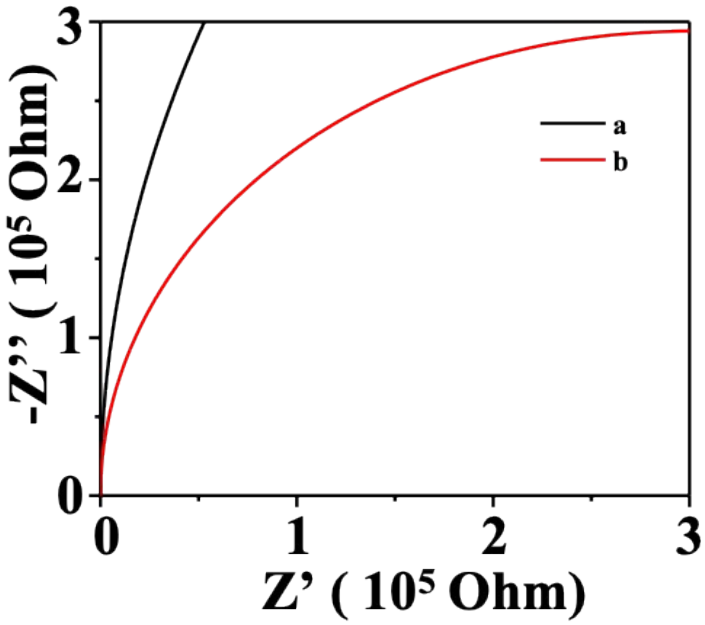

Fig. S9. Electrochemical impedance spectroscopy (EIS) of (a) the commercial P25 and (b) A_{76}/R_{24}-TiO_2 under AM1.5 irradiation

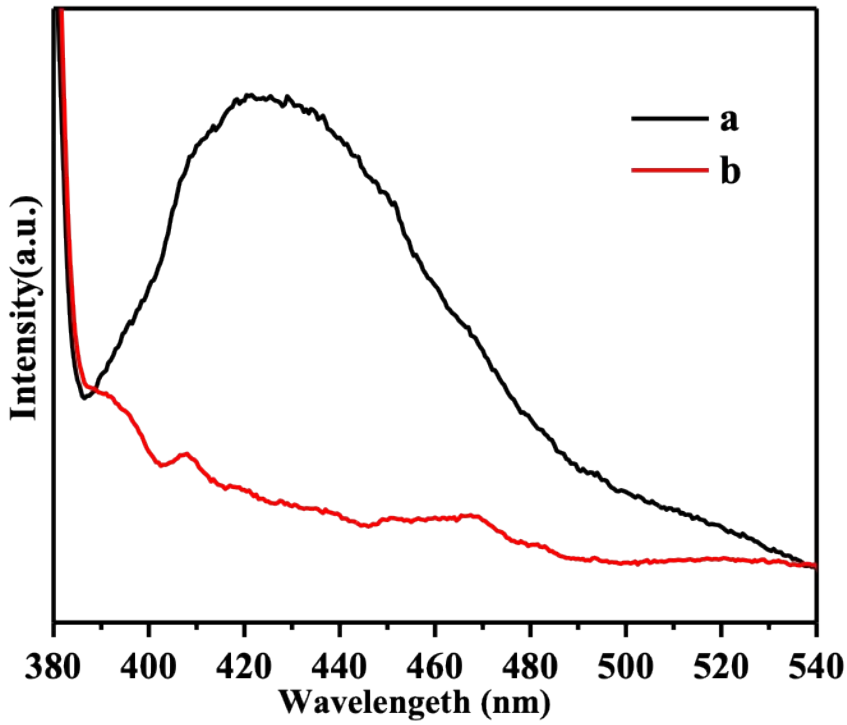

Fig. S10. The photoluminescence spectra of (a) the commercial P25 and (b) A_{76}/R_{24}-TiO_2.

3. Supplementary Tables

Table S1. Table Caption Comparison of the H_2 evolution efficiency for the TiO_2-based catalysts without using any co-catalysts.

Photocatalyst (mg)	Light source	Reactant solution	H_2 $\times 10^{-3}$ (mmol h^{-1})	Ref.
Hy-500, 20 mg	AM1.5 (100 mWcm^{-2})	11%TEOA/ H_2O	69.6	S1
blue TiO_2, 20 mg	AM1.5 (100 mWcm^{-2})	50% CH_3OH/H_2O	69.2	S2
Bi_2O_2Se/TiO_2 , 20mg	300 W Xe lamp	5%glycerol/ H_2O	24.8	S3
TiO_2@MOF FS, 10 mg	AM1.5 (100 mWcm^{-2})	8%TEOA/ H_2O	4.4	S4
TiO_2 nanorod, 5 mg	solar light	5%glycerol/ H_2O	3.535	S5
H-Graphene-TiO_2, 3 mg	150 W Xe lamp 310 < λ < 625 nm	20% CH_3OH/H_2O	3.51	S6
HC-TiO_2, 20 mg	300 W Xe lamp	10%TEOA/ H_2O	0.6608	S7
TiO_2/TiH_2, 2 mg	AM1.5 (100 mWcm^{-2})	50% CH_3OH/H_2O	0.44	S8
anatase/rutile, 2 mg	AM1.5 (100 mWcm^{-2})	50% CH_3OH/H_2O	0.43	S9
Grey TiO_2, 2 mg	AM1.5 (100 mWcm^{-2})	50% CH_3OH/H_2O	0.306	S10
A_{76}/R_{24}-TiO_2, 30 mg	AM1.5 (100 mWcm^{-2})	20% CH_3OH/H_2O	68.1	This work

Table S2. Table Caption Comparison of the H_2 evolution efficiency for the TiO_2-based catalysts with co-catalysts**.**

Photocatalyst	Light source	Reactant solution	Co-catalyst	H_2 $\times 10^{-3}$ (mmol h^{-1})	Ref
S-doped H-TiO_2, 100 mg	AM 1.5G	25% CH_3OH/H_2O	0.5% Pt	25.8	S11
Co_3O_4 QDs/TiO_2, 50 mg	AM 1.5G	10% CH_3OH/H_2O	1% Pt	86.755	S12
Ni-a/TiO_2，50 mg	300W Xe lamp	10% CH_3OH/H_2O	Atomic Ni (1.11 wt%)	94.5	S13
TiO_2 hierarchical microspheres，10 mg	AM 1.5G	10% CH_3OH/H_2O	Atomic Pt (0.36 wt%)	117	S14
Black TiO_2 microspheres，20 mg	AM 1.5G	20%CH_3OH/H_2O	1% Pt	130.8	S15
Co-TiO_2，100 mg	300 W xenon arc lamp	20% CH_3OH/H_2O	Atomic Co (1.11 wt%)	168.2	S16
Cu–TiO_2,10 mg	300 W xenon arc lamp	20% CH_3OH/H_2O	Atomic Cu (0.75 wt%)	177.7	S17
triphase anatase-rutile-brookite TiO_2，50 mg	300 W Xe arc lamp	25% CH_3OH/H_2O	1% Au	178.5	S18
Sub-10 nm rutile TiO_2 Nanoparticles, 100 mg	AM 1.5G	10% CH_3OH/H_2O	1% Pt	195.4	S19
H-TiO_2, 20 mg	AM 1.5G	50% CH_3OH/H_2O	0.6%Pt	200	S20
Hydrogenated titanate nanotube,100 mg	AM 1.5G	20% CH_3OH/H_2O	1% Pt	215	S21
TiO_2 ultrathin nanosheets，30 mg	AM 1.5G	20% CH_3OH/H_2O	1% Pt	540.69	S22
Dehiscent mesoporous rutile TiO_2，50 mg	AM 1.5G	25% CH_3OH/H_2O	1% Pt	610.8	S23
Ordered Meso-TiO_2-25 microspheres，50mg	AM 1.5G	25% CH_3OH/H_2O	1% Pt	630	S24
Al reduced H-TiO_2, 100 mg	AM 1.5G	25% CH_3OH/H_2O	0.5% Pt	640	S25
A_{76}/R_{24}-TiO_2, 30 mg	**AM 1.5G**	**20% CH_3OH/H_2O**	**1% Pt**	**562.56**	**This work**

Table S3. Comparison of methods that can modulate the composition of the TiO_2 phase.

Photocatalyst	Temperature	Pressure	Time	Materials	Cost	H_2 production with/without cocatalyst / (μmol h^{-1})	Reference
P25	1800℃	High	***	$TiCl_4$	High	131/2.415[a] (30 mg)	Degussa P25
Ordered Meso-TiO_2 -25 microspheres	400℃	Normal	~ 31 h	Pluronic F127, HCl, HOAc, TBOT, THF	Normal	630/*** (50 mg)	Chem. Sci., 2019, 10, 1664-1670.
anatase/rutile TiO_2	500℃	20 bar	1 h-3 day	TiO_2 (anatase, rutile and mixed phase), purity H_2(purity 99.999 %).	High	***/0.215 (2 mg)	Angew. Chem., Int. Ed., 2014, 53, 14201-14205
triphase anatase-rutile-brookite TiO_2	100℃	Normal	~ 38 h	HCl, HOAc, $TiCl_4$, PEI	Normal	178.5/***(50 mg)	Adv. Energy Mater., 2019, 9, 1901634
A_{76}/R_{24}-TiO_2	500℃	Normal	~ 30 h	$TiCl_4$, PVA, NMP	Low	563/68.19 (30 mg)	This work

Note: [a] The P25 photocatalytic hydrogen production values were measured in our laboratory. ***Represents a failure of the data to be found in the literature.

4. Supplemental References

S1 Y. Jiang, H. Ning, C. Tian, B. Jiang, Q. Li, H. Yan, X. Zhang, J. Wang, L. Jing and H. Fu, Single-crystal TiO_2 nanorods assembly for efficient and stable cocatalyst-free photocatalytic hydrogen evolution, *Appl. Catal., B*, 2018, **229**, 1-7.

S2 K. Zhang, L. Wang, J. K. Kim, M. Ma, G. Veerappan, C.-L. Lee, K.-j. Kong, H. Lee and J. H. Park, An order/disorder/water junction system for highly efficient co-catalyst-free photocatalytic hydrogen generation, *Energy Environ. Sci.*, 2016, **9**, 499-503.

S3 D. Ding, Z. Jiang, D. Ji, M. Nosang Vincent and L. Zan, Bi_2O_2Se as a novel co-catalyst for photocatalytic hydrogen evolution reaction, *Chem. Eng. J.*, 2020, **400**, 125931.

S4 L. Sun, Y. Yuan, F. Wang, Y. Zhao, W. Zhan and X. Han, Selective wet-chemical etching to create TiO_2@MOF frame heterostructure for efficient photocatalytic hydrogen evolution, *Nano Energy*, 2020, **74**, 104909.

S5 N. L. Reddy, D. P. Kumar and M. V. Shankar, Co-catalyst free Titanate Nanorods for improved Hydrogen production under solar light irradiation, *J. Chem. Sci. (Bangalore, India)*, 2016, **128**, 649-656.

S6 T.-D. Nguyen-Phan, S. Luo, Z. Liu, A. D. Gamalski, J. Tao, W. Xu, E. A. Stach, D. E. Polyansky, S. D. Senanayake, E. Fujita and J. A. Rodriguez, Striving Toward Noble-Metal-Free Photocatalytic Water Splitting: The Hydrogenated-Graphene-TiO_2 Prototype, *Chem. Mater.*, 2015, **27**, 6282-6296.

S7 G. Jia, Y. Wang, X. Cui and W. Zheng, Highly Carbon-Doped TiO_2 Derived from MXene Boosting the Photocatalytic Hydrogen Evolution, *ACS Sustainable Chem. Eng.*, 2018, **6**, 13480-13486.

S8 N. Liu, X. Zhou, N. T. Nguyen, K. Peters, F. Zoller, I. Hwang, C. Schneider, M. E. Miehlich, D. Freitag, K. Meyer, D. Fattakhova-Rohlfing and P. Schmuki, Black Magic in Gray Titania: Noble-Metal-Free Photocatalytic H_2 Evolution from Hydrogenated Anatase, *ChemSusChem*, 2017, **10**, 62-67.

S9 N. Liu, C. Schneider, D. Freitag, U. Venkatesan, V. R. R. Marthala, M. Hartmann, B. Winter, E. Spiecker, A. Osvet, E. M. Zolnhofer, K. Meyer, T. Nakajima, X. Zhou and P. Schmuki, Hydrogenated Anatase: Strong Photocatalytic Dihydrogen Evolution without the Use of a Co-Catalyst, *Angew. Chem., Int. Ed.*, 2014, **53**, 14201-14205.

S10 X. Zhou, N. Liu, J. Schmidt, A. Kahnt, A. Osvet, S. Romeis, E. M. Zolnhofer, V. R. R. Marthala, D. M. Guldi, W. Peukert, M. Hartmann, K. Meyer and P. Schmuki, Noble-Metal-Free Photocatalytic Hydrogen Evolution Activity: The Impact of Ball Milling Anatase Nanopowders with TiH_2, *Adv. Mater.*, 2017, **29**, 1604747.

S11 C. Yang, Z. Wang, T. Lin, H. Yin, X. Lü, D. Wan, T. Xu, C. Zheng, J. Lin, F. Huang, X. Xie and M. Jiang, Core-Shell Nanostructured "Black" Rutile Titania as Excellent Catalyst for Hydrogen Production Enhanced by Sulfur Doping, *J. Am. Chem. Soc.*, 2013, **135**, 17831-17838.

S12 J. Liu, J. Ke, Y. Li, B. Liu, L. Wang, H. Xiao and S. Wang, Co_3O_4 quantum dots/TiO_2 nanobelt hybrids for highly efficient photocatalytic overall water splitting, *Appl. Catal., B*, 2018, **236**, 396-403.

S13 M. Xiao, L. Zhang, B. Luo, M. Lyu, Z. Wang, H. Huang, S. Wang, A. Du and L. Wang, Molten-Salt-Mediated Synthesis of an Atomic Nickel Co-catalyst on TiO_2 for Improved Photocatalytic H_2 Evolution, *Angew. Chem., Int. Ed.*, 2020, **59**, 7230-7234.

S14 J. Xi, X. Zhang, X. Zhou, X. Wu, S. Wang, W. Yu, N. Yan, K. P. Loh and Q.-H. Xu, Titanium dioxide hierarchical microspheres decorated with atomically dispersed platinum as an efficient photocatalyst for hydrogen evolution, *J. Colloid Interface Sci.*, 2022, **623**, 799-807.

S15 C. Wang, X. Kang, J. Liu, D. Wang, N. Wang, J. Chen, J. Wang, C. Tian and H. Fu, Ultrathin black TiO_2 nanosheet-assembled microspheres with high stability for efficient solar-driven photocatalytic hydrogen evolution, *Inorg. Chem. Front.*, 2023, **10**, 1153-1163.

S16 X. Wu, S. Zuo, M. Qiu, Y. Li, Y. Zhang, P. An, J. Zhang, H. Zhang and J. Zhang, Atomically defined Co on two-dimensional TiO_2 nanosheet for photocatalytic hydrogen evolution, *Chem. Eng. J.*, 2021, **420**, 127681.

S17 Y. Ma, Y. Zhang, Y. Ma, T. Lv, B. Xiao, X. Kuang, X. Deng, J. Zhang, J. Zhao and Q. Liu, *In situ* Cu single atoms anchoring on MOF-derived porous TiO_2 for the efficient separation of photon-generated carriers and photocatalytic H_2 evolution, *Nanoscale*, 2022, **14**, 15889-15896.

S18 H. Xiong, L. Wu, Y. Liu, T. Gao, K. Li, Y. Long, R. Zhang, L. Zhang, Z.-A. Qiao, Q. Huo, X. Ge, S. Song and H. Zhang, Controllable Synthesis of Mesoporous TiO_2 Polymorphs with Tunable Crystal Structure for Enhanced Photocatalytic H_2 Production, *Adv. Energy Mater.*, 2019, **9**, 1901634.

S19 L. Li, J. Yan, T. Wang, Z.-J. Zhao, J. Zhang, J. Gong and N. Guan, Sub-10 nm rutile titanium dioxide nanoparticles for efficient visible-light-driven photocatalytic hydrogen production, *Nat. Commun.*, 2015, **6**, 5881.

S20 X. Chen, L. Liu, P. Y. Yu and S. S. Mao, Increasing Solar Absorption for Photocatalysis with Black Hydrogenated Titanium Dioxide Nanocrystals, *Science*, 2011, **331**, 746-750.

S21 Z. Zheng, B. Huang, J. Lu, Z. Wang, X. Qin, X. Zhang, Y. Dai and M.-H. Whangbo, Hydrogenated titania: synergy of surface modification and morphology improvement for enhanced photocatalytic activity, *Chem. Commun. (Cambridge, U. K.)*, 2012, **48**, 5733.

S22 S. Hu, P. Qiao, L. Zhang, B. Jiang, Y. Gao, F. Hou, B. Wu, Q. Li, Y. Jiang, C. Tian, W. Zhou, G. Tian and H. Fu, Assembly of TiO_2 ultrathin nanosheets with surface lattice distortion for solar-light-driven photocatalytic hydrogen evolution, *Appl. Catal., B*, 2018, **239**, 317-323.

S23 K. Lan, R. Wang, W. Zhang, Z. Zhao, A. Elzatahry, X. Zhang, Y. Liu, D. Al-Dhayan, Y. Xia and D. Zhao, Mesoporous TiO_2 Microspheres with Precisely Controlled Crystallites and Architectures, *Chem*, 2018, **4**, 2436-2450.

S24 W. Zhang, H. He, Y. Tian, K. Lan, Q. Liu, C. Wang, Y. Liu, A. Elzatahry, R. Che, W. Li and D. Zhao, Synthesis of uniform ordered mesoporous TiO_2 microspheres with controllable phase junctions for efficient solar water splitting, *Chem. Sci.*, 2019, **10**, 1664-1670.

S25 Z. Wang, C. Yang, T. Lin, H. Yin, P. Chen, D. Wan, F. Xu, F. Huang, J. Lin, X. Xie and M. Jiang, Visible-light photocatalytic, solar thermal and photoelectrochemical properties of aluminium-reduced black titania, *Energy Environ. Sci.*, 2013, **6**, 3007.